



**European volcanological supersite in Iceland:
a monitoring system and network for the future**

Report

D7.1 - Eruption Instruments and Plume Models

| | | |
|------------------------------|---|--|
| Work Package: | <i>Determination and evolution of eruption source parameters</i> | |
| Work Package number: | 7 | |
| Deliverable: | <i>Eruption Instruments and Plume Models</i> | |
| Deliverable number: | D7.1 | |
| Type of Activity | RTD | |
| Responsible activity leader: | <i>Magnús Tumi Guðmundsson</i> | |
| Responsible participant: | IMO | |
| Authors: | <i>Halldór Björnsson (IMO)</i> <i>Mark Woodhouse (UNIVBRIS)</i> <i>Maurizio Ripepe (UNIFI)</i> <i>Bernd Zimanowski (UNIWUE)</i> <i>Alessandro Aiuppa (UNIPA)</i> <i>Guðmunda M Sigurðardóttir (IMO/UI)</i> <i>Bo Galle(Chalmers)</i> <i>Þórdís Högnadóttir (UI)</i> <i>Sibylle von Löwis of Menar(IMO)</i> <i>Thomas Walter (GFZ)</i> <i>Bergur H. Bergsson.(IMO)</i> | |
| Type of Deliverable: | <i>Report</i> [X] <i>Prototype</i> [] | <i>Demonstrator</i> [] <i>Other</i> [] |
| Dissemination level: | <i>Public</i> [x] <i>Prog. Participants</i> [] | <i>Restricted Designated Group</i> [] <i>Confidential (consortium)</i> [] |



Abstract

As part of the FP7 FutureVolc project Work Package 7 (WP7) uses a multi-parameter approach to assess the source parameters of a volcanic eruption. To this end several types of instruments are set up, and their output is integrated with modelling results in order to obtain best estimates of source parameters and the uncertainty in these estimates.

This report discusses eight different types of instruments, as well as methods of analysis and modelling. It is the first deliverable in Work Package 7 of project.

Contents

| | |
|---|----|
| Abstract | i |
| 1 Introduction..... | 3 |
| 2 Instruments installed | 4 |
| 2.1 Radar network..... | 4 |
| 2.2 Mobile Radiosonde..... | 6 |
| 2.3 Infra sound..... | 6 |
| 2.4 Electric field sensors..... | 8 |
| 2.5 A Quick-deployment gas monitoring system | 10 |
| 2.6 A quick deployment Scanning mini-DOAS instrument for gas emission monitoring | 12 |
| 2.7 Optical Particle Sizer | 15 |
| 2.8 Cameras | 17 |
| 3 Improvements in analysis and modelling..... | 19 |
| 3.1 Lightning based Operational Real time Eruption Location system (OREL)..... | 19 |
| 3.2 Analysis of motion in the Eyjafjallajökull plume..... | 23 |
| 3.3 Advances in plume modeling | 26 |
| 3.4 PlumeRise – an operational webtool for plume modelling | 28 |
| 4 References..... | I |

1 Introduction

This report is the first deliverable in Work Package 7 of the FP7 FutureVolc project. This WP deals with observations and modelling of volcanic plumes as they rise in the atmosphere. The WP aims to use a multi-parameter approach to estimate the mass flow rate from the volcano, and other volcanological parameters relevant to hazard management. By employing several methods of observation and different plume models, the goal of the WP is to reduce the large uncertainty associated with current methods for the determination of the flow rate from an explosive eruption.

In the FutureVolc Description of Work (DOW) this deliverable is described in the following manner:

Eruption instruments and plume models: Report on instrument installations in the field for determination of eruption source parameters; Report on new plume height magma discharge correlations and models (delivered to WP8) and new automatic algorithms for eruption plume detection based on lightning data

We break the discussion into two main sections, one on the instruments that have been set up, another on the efforts of analysing data and the modelling of volcanic plumes.

2 Instruments installed

In total 8 types of instruments have been installed in the field, or are ready to be operationally deployed, as part of FutureVolc. This section discusses each type of instrument briefly.

2.1 Radar network

The IMO C-band weather radar stationed at the international airport in Keflavik has, for more than two decades, been the principal all-weather remote sensing tool for monitoring eruptions in Iceland. The radar was installed in 1991 and it was first used to monitor the eruption of Hekla in 1991, only a few days after the radar became operational. It was subsequently used during the eruptions of Gjalp in 1996, Grímsvötn in 1998, Hekla in 2000, Grímsvötn in 2004, Eyjafjallajökull in 2010 and Grímsvötn in 2011. Coincidentally, all eruptions in Iceland since the installation of the radar at Keflavik were within the area covered by the radar, although Grímsvötn is close to the edge of that domain. In 2012 the IMO installed another C-band radar near Teigsbjarg in the east of Iceland allowing for a more complete coverage of volcanoes in Iceland (Figure 1). Furthermore, the IMO has bought two mobile X-band weather radars, with funding from ICAO, which can be used to monitor volcanic activity from a suitable distance. This strategy was used during the eruption of Grímsvötn in 2011 utilizing a mobile X-band radar that was on loan from the Italian civil protection authorities (Figure 2).

One of the X-band radars is currently stationed at Gunnarsholt in South Iceland within view of active volcanoes (including Hekla, Eyjafjallajökull and Katla), but this radar can and will be moved if necessary. During the summer of 2013 IMO radar operators used the other X-band radar to examine several potential sites for mobile radar deployment (Figure 3). The sites were located all over Iceland, and their selection was based on a list of active volcanoes.

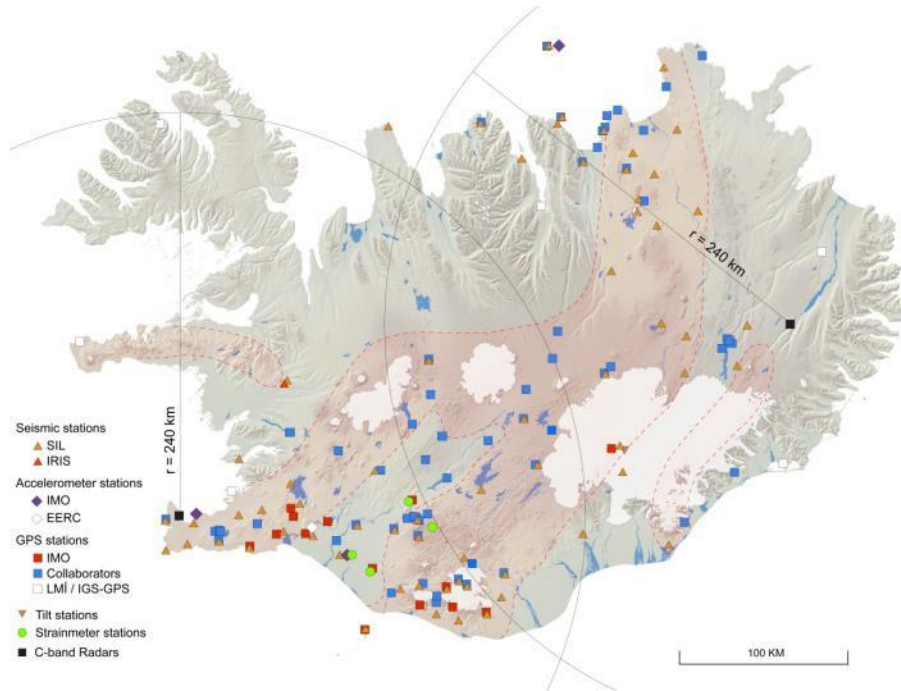


Figure 1 The location of fixed C-band weather radars and some of the instruments run by the IMO. Both radars can be extended to more than the 240 km range. The X-band mobile radars have a shorter range but can see smaller particles.

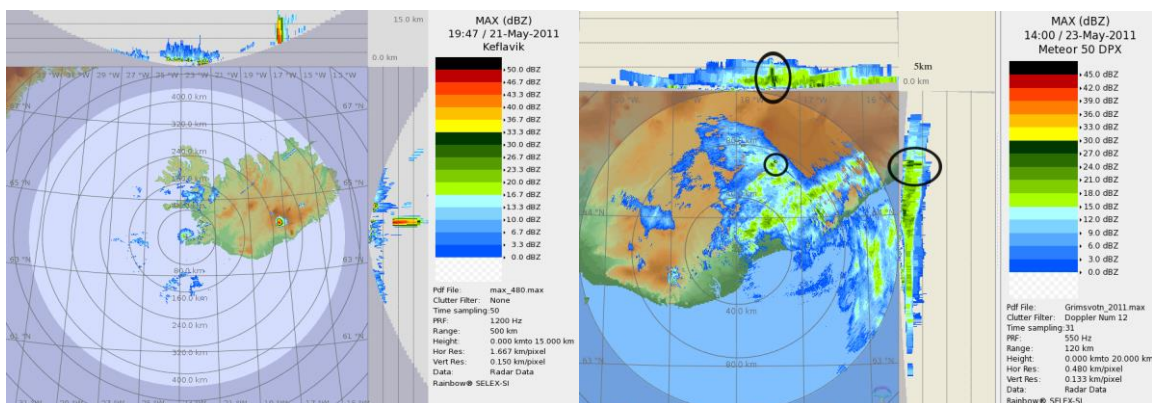


Figure 2 Radar images from the Grímsvötn 2011 eruption, from the C-band radar in Keflavik and the X - band radar located at about 80km from the eruption



Figure 3 One of the new mobile X-band radars being deployed operationally.

2.2 Mobile Radiosonde

Models of volcanic plumes require information about the temperature, wind and humidity profile above the volcano. Inaccuracies in input meteorology, for example from using atmospheric soundings taken far from the volcano or using NWP data, can lead to errors in the model predictions that are difficult to quantify. Currently there are only two sites in Iceland where atmospheric radiosonde measurements are done, twice per day at Keflavik and once per day Egilsstaðir. To monitor the evolution of the atmospheric parameters closer to the volcano, a mobile radiosonde system was bought from Vaisala in 2012. This system has been tested in the field on several occasions and in August 2013 it was used with a special instrument package consisting of a cloud detection sensor and a geiger counter (Figure 4).



Figure 4 Radiosonde release bay and experimental release of a radiosonde in August 2013. The instrument package contains both the standard instruments, and also an experimental science package (cloud detection and gamma rays) designed by the University of Reading, UK

2.3 Infra sound

Volcano infrasound is effective for tracking and quantifying eruptive phenomena because it corresponds to activity occurring near and around the volcanic vent, in contrast to seismic signals that are generated by both surface and internal volcanic processes. Infrasound can be recorded remotely and is not heavily dependent on good weather conditions or daylight. Thus,

infrasound can provide a continuous record of a volcano's unrest. Moreover, it can be exploited at regional or global distances. Infrasound is measured with a specifically designed network of sensors (array), which allows the signal-to-noise ratio to be improved, and reduces the ambiguity of signal detection. The sensors are arranged in a “star” geometry with 200 m of aperture, with each sensor linked to the receiver by a fibre optics cable (Figure 5 and 6). As part of FutureVolc a network of three infrasonic arrays will be deployed in the southern volcanic area of Iceland at distances ranging from 30 km to 80 km from the main active volcanoes. On June 12 – 21 2013 an infrasound array was deployed in a forest at Sandartunga, approximately 18 km North-West of Hekla (Figure 5). The data from the array (Figure 7) is transmitted to IMO and Italy, and can be analyzed and processed in real time. This array complements a pre-existing array placed in Gunnarsholt, southern Iceland. During a volcanic eruption the infrasound data can be used to calculate plume exit velocity and volumetric flux in real-time. These parameters can be integrated into models of near-source plume motion and will improve our understanding of the dynamics of volcanic plumes.

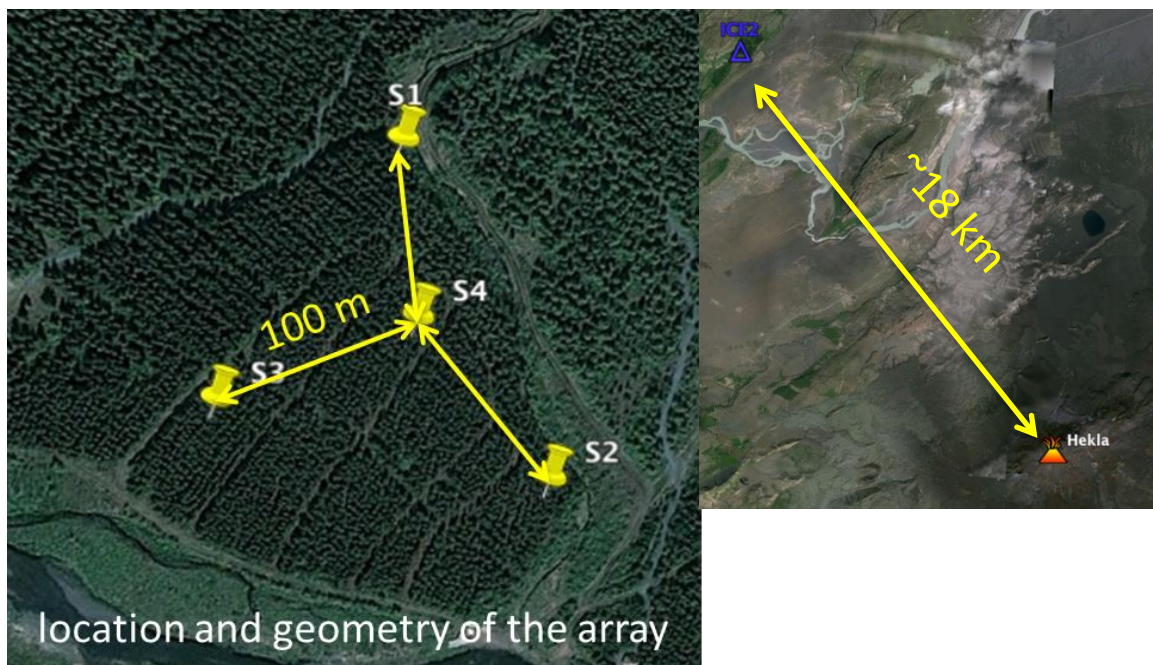


Figure 5 Geometry of the array. It has 4 elements and aperture of 150 m. Each element is linked to the central station by a 100 m long fibre optics cable. Data acquisition is at 16 bits with a sampling rate of 50 Hz. Data are radio transmitted by GPRS link to Italy and IMO.



Figure 6 Central station (left) and Pressure sensor (right). Each sensor contains a differential pressure transducer sensitive up to 100 Pa with 25 mV/Pa resolution. Pressure is digitized at 180 Hz and then transmitted with information on internal temperature and battery voltages. Power consumption is 20 mA @12 V

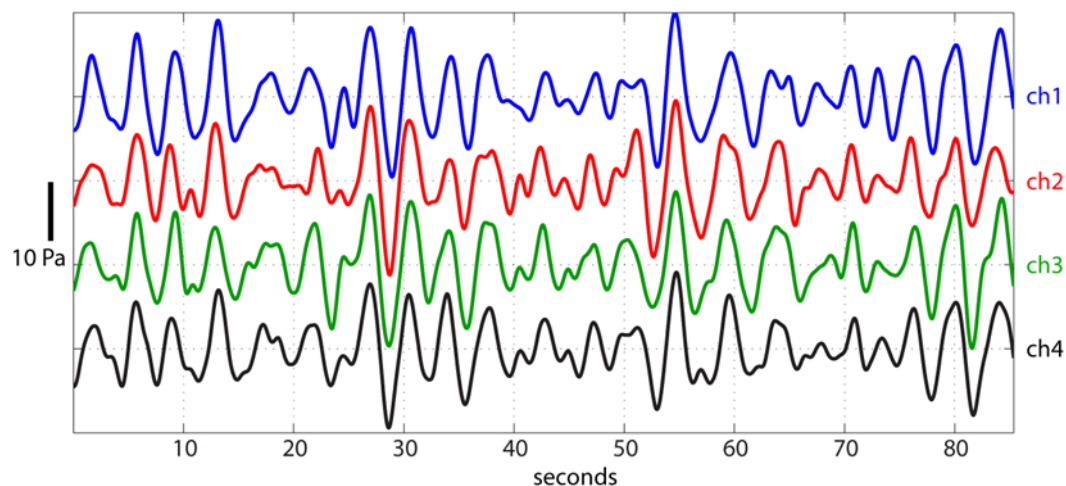


Figure 7 The data from the array is transmitted to IMO and Italy, and can be analyzed and processed in real time. During a volcanic eruption the infrasound data can be used to calculate plume exit velocity and volumetric flux in real-time.

2.4 Electric field sensors

Explosive eruptions cause very strong variations of the atmospheric electrical potential gradient. The observed fluxes in this gradient are useful to discriminate between magmatic eruption pulses, that produce fluxes in the range 10 to 100 V/(m*s), and phreatomagmatic

ones, that give fluxes in the range 10^3 to 10^4 V/(m*s). A linear correlation between the new surface area generated by the formation of volcanic ash, the kinetic energy release, and the intensity of the electric signal, allows for the quasi- real-time monitoring of the energy released and the mass of tephra produced, using models or measurements of the grain-size distribution of the tephra.

Within FutureVolc, three fixed electrical stations (at Grimsvötn, Hekla, and Katla) will operate, and one mobile system for the eruptions at other volcanoes is at the disposal of IMO. All electronics and hardware parts of the e-field stations have been produced and pre-calibrated. The electronic circuitry was optimized and ruggedized to meet the requirements for long-term operation under cold and moist conditions. During the summer and autumn of 2013 all the equipment was delivered to IMO, the installation sites inspected, and the background noise measured (Figure 8 and 9). The fixed stations are located at Grímsfjall (Grimsvötn), Feðgar (Hekla), and Slysaalda (Katla). The instruments have been installed and data relay issues are being worked on.

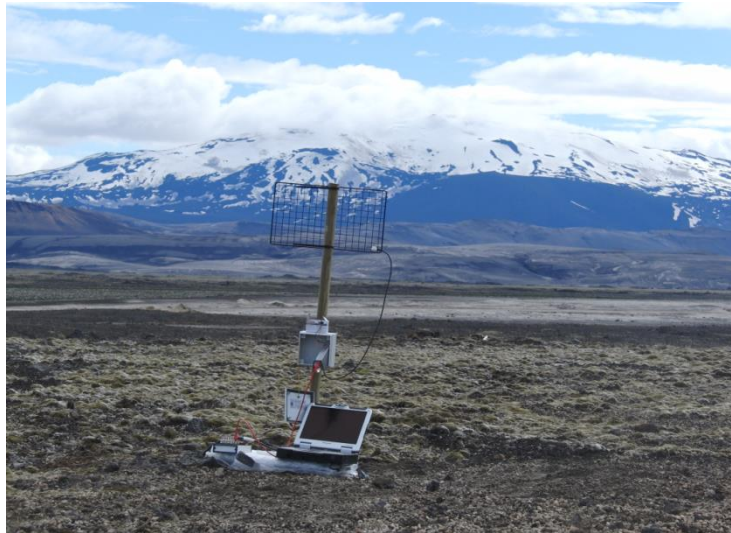


Figure 8 Test station near Ísakot in front of Hekla volcano, approx.10 km from the top of the volcano.

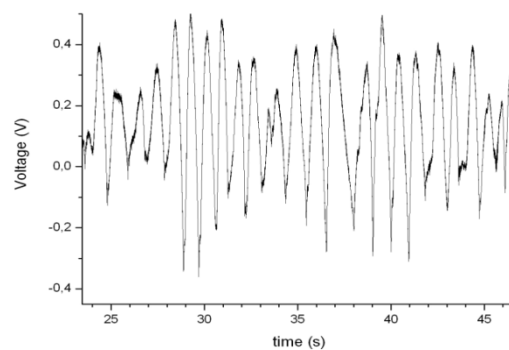


Figure 9 Noise caused by the blades of two wind power stations recorded near Ísakot GPS Station

2.5 A Quick-deployment gas monitoring system

Within FutureVolc, a gas monitoring system has been developed that can be rapidly deployed (within 1 day) at volcanoes starting to show signals of unrest, or where an eruption has commenced. During an ongoing eruption, the measurements from the system will allow quantification of the total volatile flux, and independent estimates of magma degassing budgets.

The quick-deployment portable version of the MultiGAS (Multi-component Gas Analyzer System) instrument was developed by UNIPA and delivered to IMO in May 2013. This fully-automated instrument (Figure 10) is designed to measure (at 0.1 Hz rate) the concentrations of major volcanic gas species (H_2O , CO_2 , SO_2 , H_2S) in a volcanic gas plume, and integrates (i) an infrared spectrometer for CO_2 sensing (Gascard II, calibration range 0 – 3000 ppmv; accuracy $\pm 2\%$, resolution, 0.8 ppmv); (ii) two specific electrochemical sensors for measurement of SO_2 (CityTechnology, sensor type 3ST/F, calibration range, 0 - 200 ppmv, accuracy, $\pm 5\%$, resolution, 0.1 ppmv) and H_2S (SensoriC, sensor type 2E, calibration range, 0 – 200 ppmv, accuracy, $\pm 5\%$, resolution, 0.1 ppmv); and (iii) temperature, pressure and relative humidity (Galltec sensor, measuring range, 0 – 100 % Rh, accuracy, $\pm 2\%$) sensors for calculation of H_2O concentrations.

The system is fully operative, and can be deployed rapidly (within 1 day) at volcanic systems which have started showing independent signals of unrest, or when an eruption has commenced. To test its performance, UNIPA and IMO have since June 2013 been operating the instrument in the field (at Grímsfjall and Sveinstindur), first to measure the baseline gas-ratios of Grímsfjall (Figure 10) and secondly to explore the possibility of detecting precursory gas signals to an expected flood (jökulhlaup).

The station consists of a very rugged and strong case (Peli case) housing the MultiGAS instrument, two 100 Ah batteries, power cables and communication devices (a 3G modem or a



Figure 10 Interior of the portable MultiGAS and the station at work on Grímsfjall (05/06/2013)

radio-link). Batteries can keep the station running autonomously for about 30 days (depending on the interval of measurements); powering by either a solar panel or a wind generator is also

possible. The station has full telemetry capability with two possible options, through a 3G/GPRS router or freewave radios.



Figure 11 The MultiGAS at Sveinstindur. Left: Radio receiver setup. Right: MultiGas with solar panel.

IMO has assisted deployment by providing equipment for telemetry (Figure 11), but an independent radio-link for the station will soon be integrated by UNIPA by setting up a remote receiver. The station was tested twice during the summer of 2013, on Grímsfjall and Sveinstindur. On Grímsfjall, the station ran autonomously for 5 days and data was successfully gathered during the days of the campaign with no maintenance problems.

Currently, the instrument has been deployed at Sveinstindur (Figure 11), in collaboration with the IMO, with the objective of detecting any anomalous gas signal related to the expected jökulhlaup from Skaftárkatlar down Skaftá. The station was set up with a radio-link and has been functioning regularly and with no interruptions (and is still waiting for the jökulhlaup). The instrument can be controlled remotely and set up to perform 1 to 12 daily measurement cycles of 30 minutes each. During each cycle, the plume gas is continuously pumped into the sensors' housing; a data-logger board captures the output signals from the sensors at 0.1 Hz rate. The receiver unit consists of a protective case sheltering a battery, the second radio and a modem (router), plus a portable mast (with two antennas) along with a wind generator or solar panel (Figure 11).

The Multi-GAS instrument is fully operational and should guarantee rapid field deployment at most locations with nearly real-time data transmission.

2.6 A quick deployment Scanning mini-DOAS instrument for gas emission monitoring

Another quick-deployment system used within FutureVolc is a modified NOVAC Scanning DOAS instrument described in D5.3 that is adapted to be quickly deployed at any Icelandic volcano in case of an imminent eruption. Two modes of operation are facilitated; normal flux measurements providing emission estimates with 5 minutes time resolution and fast sensitive slant column measurements indicating the onset of gas emission without quantifying the emission rate. It should be possible to install the instrument within one day and deliver SO₂ emission rates with 5 minutes time resolution in real time, provided the meteorological conditions are suitable and that the volcanic activity (ash and condensed water) does not hamper the measurements.

The standard NOVAC instruments have proven to work well at low- and mid-latitudes and today 64 instruments are running on 24 volcanoes worldwide. However, so far there is only limited experience of running these instruments at high latitudes. Two major problems may be anticipated:

1. Low UV light conditions. During summer the days are long at high latitudes, but the Solar Zenith Angle is relatively large which reduces the UV-component of the scattered sunlight. In addition the higher stratospheric ozone levels in the polar vortex further reduces the UV light. During winter the high Solar Zenith Angle and short daylight duration minimizes the hours available for measurements.
2. The harsh weather conditions, especially the freezing/thawing conditions during spring and fall, may cause problems with external moving parts, such as the rotating hood of the standard NOVAC version I system.

To address these problems, two major changes have been made; (i) change to a more UV-sensitive spectrometer, and (ii) modification of the scanning device to avoid external moving parts. These developments are described in more detail in D5.3.

The modifications to a standard NOVAC instrument consist of replacing the standard OceanOptics SD2000 spectrometer with the more UV sensitive spectrometer MayaPro2000, as well as using a closed scanner with a cylindrical quartz tube replacing the rotating hood with window. A further modification is that a cylindrical lens is implemented in the optical system. This changes the field-of-view (FOV) of the instrument to become rectangular instead of circular, covering the full 7.2° angle used as scan interval. Using a fixed exposure time of 150 ms and co-adding 15 spectra results in a total time of 2 minutes to complete a scan.

The instrument has been tested on a field campaign in Alaska in July-September 2013. This campaign offered a possibility to test the instrument under realistic conditions, a high latitude location with a degassing volcano. The instrument was installed at the Martin volcano (N 58.16642°, W 115.35380°, alt 1727 m), about 3 km north of the crater and data was

downloaded from a base camp site about 14 km away using FreeWave FGR2-PE-U 900 MHz transceivers. The installation at Martin volcano is shown in Figure 12 and an example of a scan made with this instrument, yielding 76.5 ton/day SO₂ is shown in Figure 13.



Figure 12 The quick deployment Scanning DOAS installed at the Martin volcano in Alaska.

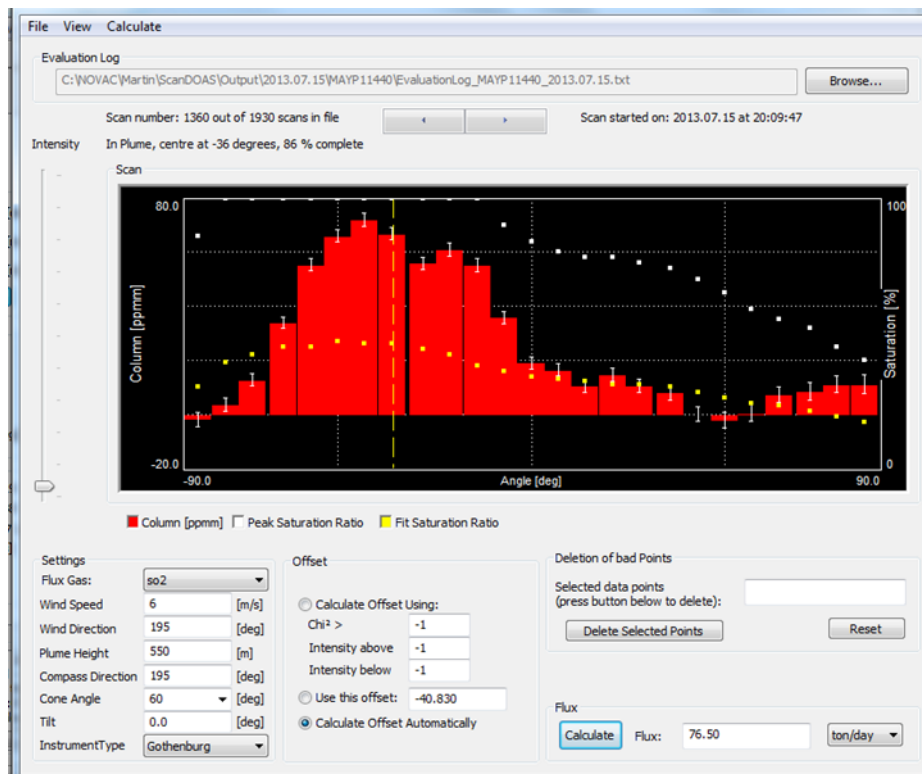


Figure 13 . Example of a measurement made by the Scanning DOAS instrument at Martin volcano on 15 July 2013. The red columns represent the vertical columns of SO₂ in a scan from one horizon to the other. The scan started at 12.09 and the SO₂ flux was evaluated to 76.5 ton/day. White and yellow dots show spectrum max intensity and fit interval intensity respective. The white bars indicate spectral evaluation error.

As it is possible that the onset of SO₂ gas emission may be an early indicator of increased activity it was decided that an alternative mode of operation of the instrument that can provide measurements of SO₂ integrated over specific areas, with high sensitivity and time resolution but without quantifying the emission, should be implemented. Thus, the Quick Deployment system can be operated in an alternative mode where it is constantly measuring the slant column of SO₂ in a fixed direction with the purpose of simply detecting the presence of SO₂.

In this mode of operation, the instrument will have a rectangular FOV covering 0.5° × 7.2°. A first test of this mode of operation was made in Alaska in July 2013, and Figure 14 shows the detection limit for SO₂ as a function of time on a day with moderate cloud cover. It can be seen that between 09.00 and 19.00 a detection limit below 5 ppmm is achieved. Note that Solar noon occur at 14.00 in Alaska.

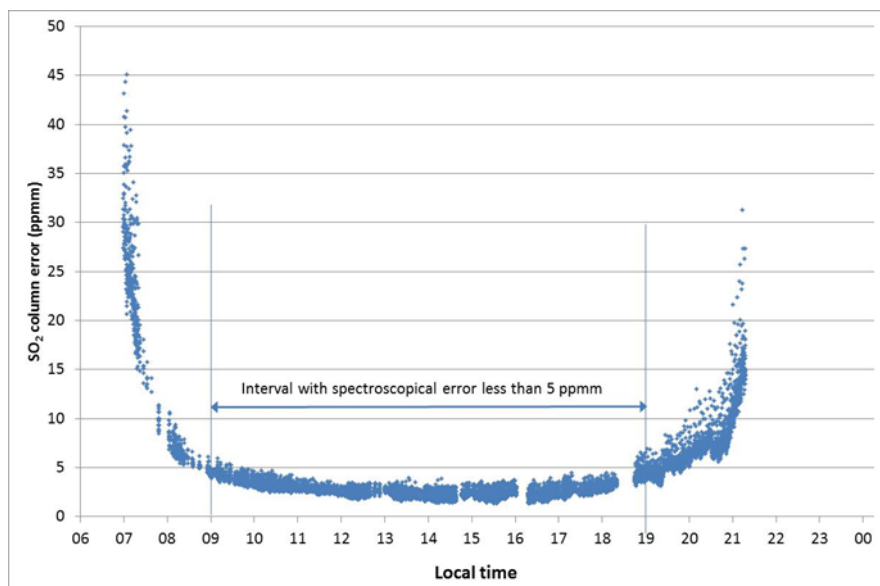


Figure 14 The error in the spectral evaluation plotted against time of day for the measurements Martin volcano on 15 July 2013. Between 09.00 and 19.00 the error is less than 5 ppmm.

The system was installed at Rauðaskál, co-located with a stationary Scanning DOAS system in September 2013 in connection with the First Annual meeting. The instrument integrates all SO₂ molecules along a rectangular FOV located just above the rim of the volcano as seen in Figure 15 and Figure 16. Data is collected with a time resolution of 10 seconds and can be downloaded in near real time to IMO via a hub at Búrfell, located 5 km north of Hekla. As the prevailing wind direction at Hekla is from southwest it can be expected that a possible SO₂ plume is intersected along a considerable distance, yielding a very good sensitivity to the presence of SO₂. As an example, if the plume is intersected over 1 km we will be able to detect concentrations as low as 5 ppb if the weather conditions are favourable. Development of a software routine for automatic real-time download and display of data is planned for fall 2013.



Figure 15 Areal photograph of Hekla and surrounding locations. The DOAS system is located at Rauðaskál, and the data is relayed to the IMO station at Búrfell.

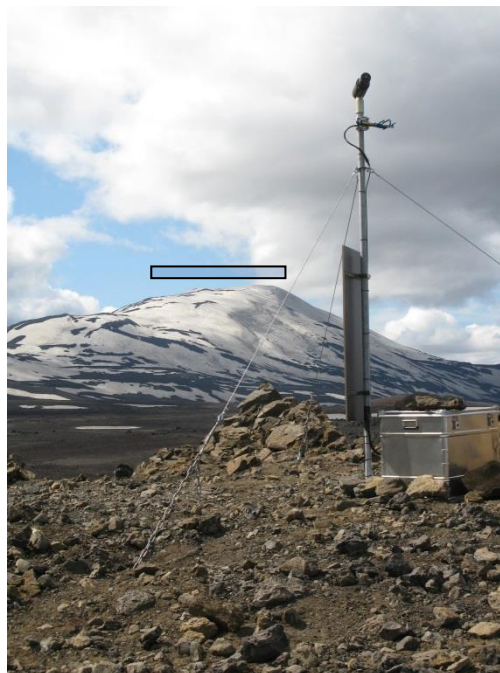


Figure 16 Hekla viewed from the Raudaskal site. A rectangle representing the Field of View of the Fast Response DOAS system is shown over the rim of Hekla.

2.7 Optical Particle Sizer

In order to obtain the concentration and size distribution of airborne particles two Optical Particle Sizers (OPS) from TSI have been acquired by IMO. An OPS operates on the principle of optical scattering from single particles. Particle pulses are sized and binned in up to 16

different channels. This instrument provides a fast and an accurate measurement of particle concentrations and particle size distributions using single particle counting technology.

Particles with optical diameters from 0.3 to 10 micrometers can be detected. The instruments, acquired for the FutureVolc project, are used to measure the particle size distribution and concentration of re-suspended ash, and will also be used to measure these properties of volcanic ash during an eruption.

One instrument was tested in a field setting for two months in summer 2013 at Svartárfkot in northeast Iceland (Figure 17), and is now installed in Fljótshverfi, east of Kirkjubæjarklaustur. The second instrument was taken into the highlands on two fieldtrips in August 2013 with the aim of measuring particle size distributions and concentrations of re-suspended sand and dust during dust storm events.



Figure 17 The OPS instrument in a field setting at Svartárfkot during 2013.

At Svartárfkot and Fljótshverfi, the OPS instruments have been connected to electricity supplies through outdoor cable into houses of local farmers. Communication with an instrument is via a mobile modem that is placed in the environmental enclosure. Some difficulties have been encountered in obtaining files on demand from the instrument, but real time data streaming to IMO is operational. The streamed data consists of total counts from each channel over a time certain period (Figure 18).

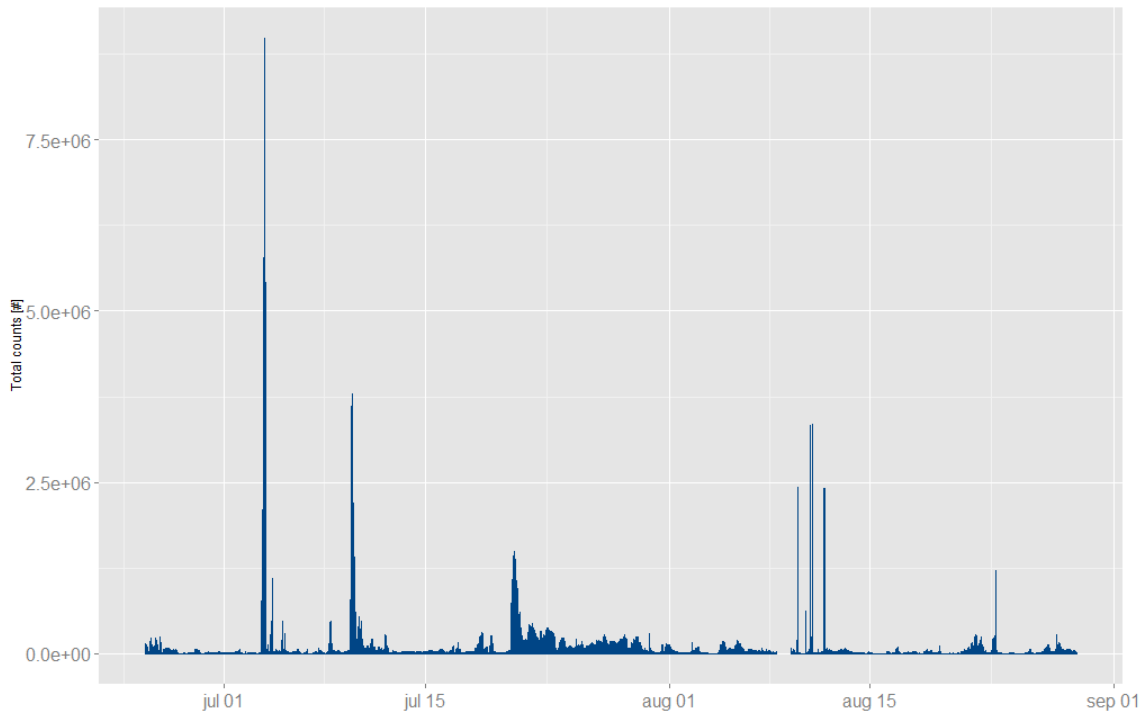


Figure 18 Total particle counts (of particles with diameter 0.3-10 μm) made with the OPS at Svartárkot NE-Iceland from 25th June to 29th of August 2013. Particles are counted over 10 minute periods. The maximum sum of total counts over ten minutes were 8980591 particles on the 3rd of July and the minimum sum of total counts were 242 particles on the 4th of August.

The instrument is relatively easy to install and set up for long-term measurements. It is portable and easy to handle to, allowing brief observations on many sites to be made, and does not need to be constantly connected to a supply of electricity. It has internal battery that lasts up to 6-12 hours. The interface is user friendly and raw data are displayed directly on the screen.

2.8 Cameras

Visual observations of volcanoes provide amongst the strongest and most widely used information of eruption occurrence, plume height or other indicators of unrest. By using fixed streaming and time lapse camera installations, FutureVolc will systematically acquire high resolution images of eruptions and further analyse them using photogrammetric approaches. Cameras will be installed and image correlation techniques will be implemented for the study of eruption source parameters such as vent location, vent motion and exit velocity at selected volcanoes.

The systems consist of a streaming camera connected to internet via radio. The image quality, compression and frame rate is controlled and held flexible depending on the activity level of the targeted volcano. Through digital flow algorithms, the systematic changes of pixels is analysed.

Three cameras have already been installed; one failed, and two are continuously operating at Mjóaskarð and Rauðaskál (Figure 19 - Figure 20). Both operational cameras have a real-time link to the IMO. Exact locations of the cameras can be seen in Figure 15.

In conjunction with the new cameras, improvements have been made to algorithms for analysing the image data, as described in the analysis section below.

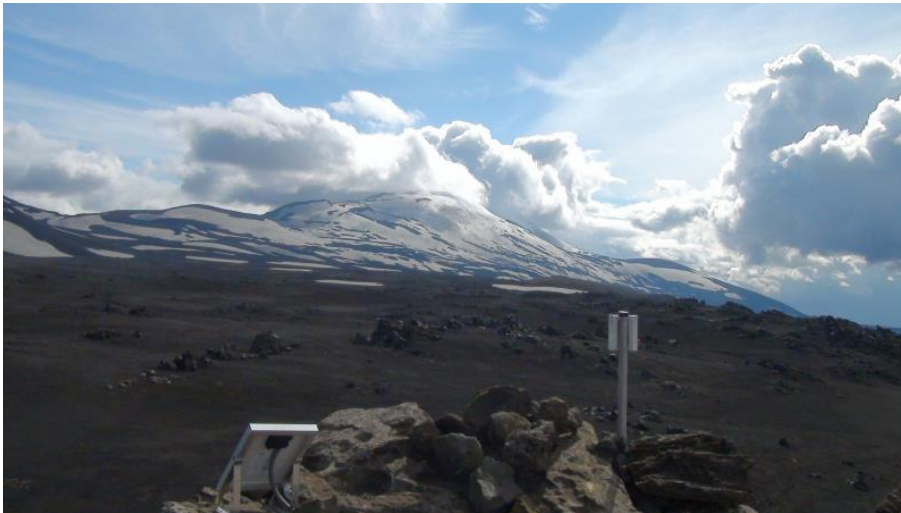


Figure 19 View from camera at Rauðaskál

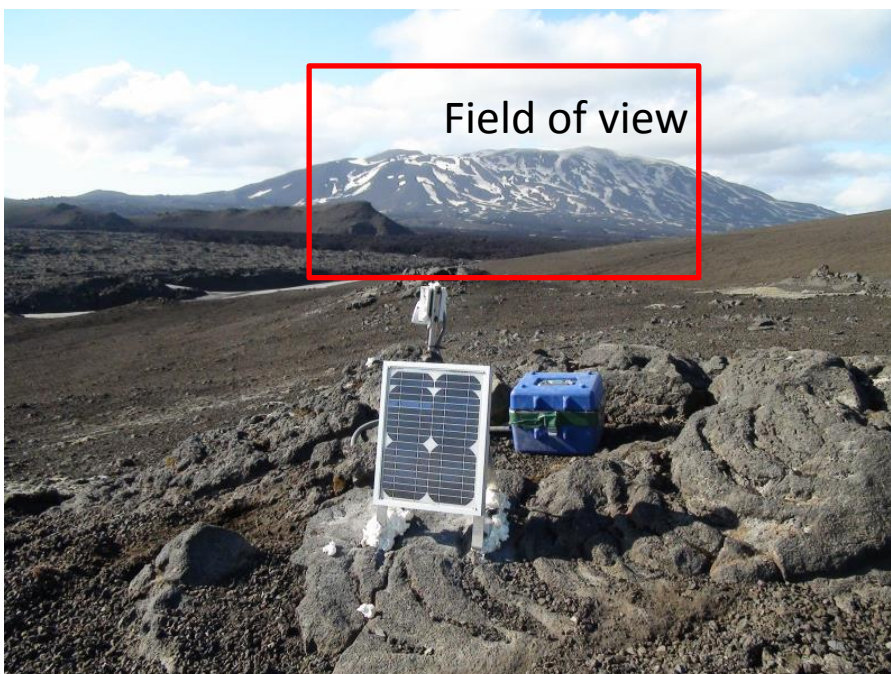


Figure 20 View from camera at Mjóaskarð.

3 Improvements in analysis and modelling

The previous section gave an overview of FutureVolc instrumentation in WP7. This section will discuss analysis and modelling efforts made as part of the consortium. These activities range from an improved use of lightning data to locate the source of an eruption and the analysis of eruption data, to new models for volcanic plumes.

3.1 Lightning based Operational Real time Eruption Location system (OREL)

During the early phase of an eruption, knowing the precise location of the vent can be very important for civil protection authorities. However, this knowledge is not always available, due to bad weather, night time conditions or other lack of visibility. Subglacial volcanic eruptions in Iceland tend to be accompanied by early lightning activity in the volcanic eruption column.

Lightning location systems, designed for weather thunderstorm monitoring, are based on remote detection of electromagnetic waves from lightning and can provide valuable real-time information on the location of an eruption site. An important aspect of such remote detection is its independence of darkness and weather, apart from thunderstorms occurring close to the volcano. However, the fact that individual lightning strikes can be over 10 km in length and are sometimes tilted and to the side of the volcanic column must be taken into account. This adds to the lightning location uncertainty, which is often a few km. Furthermore, the volcanic column may be swayed downwind (e.g. Figure 21). Therefore, the location of a single lightning event can be misleading but by calculating the average location of many lightning strikes and applying correction to account for wind a more accurate eruption site location estimate can be obtained.

A prototype of an automatic system at the IMO has been developed that analyses such real-time lightning location data and predicts the eruption site location.



Figure 21 Plume lightning during the Eyjafjallajökull 2010 eruption. The plume was blown southward (to the right on this photo) by strong northerly winds. The location of this lightning is far from the eruption site. Photo (Þórður Arason) taken from a distance of 72 km on 17 April 2010 at 04:47:09 UTC (30 s exposure time).

The electromagnetic wave from a lightning event can be observed over great distances (>10000 km). The web site of the IMO includes lightning information from the ATDnet system (Arrival Time Difference network) of the UK Met Office. This system is based on several stations in and around Europe, and has been operational since 1988 (Figure 22). One of the ATDnet stations, at Keflavík airport in Iceland, is supported by the IMO.

The stations operate in the very low frequency (VHF) range (13.7 kHz) and record the arrival time with great accuracy. Data from at least four stations are needed to locate a lightning event. The ATDnet system observes both intracloud and cloud-to-ground lightning but, because it observes variations in the local vertical electric field, the system is more susceptible to vertical (cloud-to-ground) lightning. Detailed descriptions of the ATDnet system and its use in monitoring volcanic lightning is given by Gaffard et al. (2008), Bennett et al. (2010), and Arason et al. (2011). Below, a brief description of how lightning locations could have been used to determine the location of the vent during the Grímsvötn 2011 eruption is given, followed by a brief description of the OREL system.

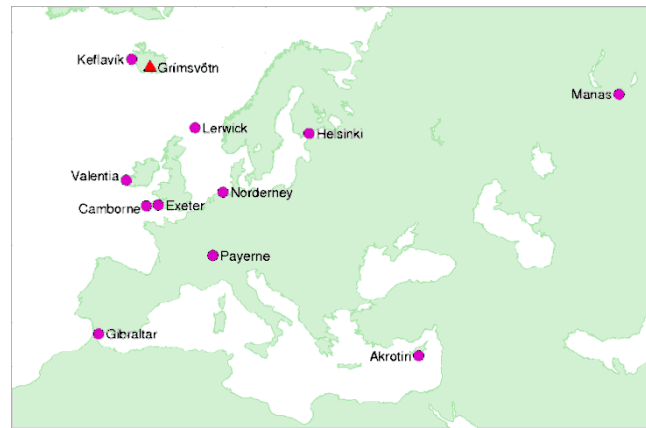


Figure 22 The stations of the ATDnet system that were in operation during the Grímsvötn 2011 volcanic eruption.

The Grímsvötn 2011 eruption started at about 19:00 UTC on 21 May. From its start it was known to be within the Grímsvötn caldera, but its specific location within the caldera could not be identified before dark. No eye witnesses were on site, and seismic data, GPS-data, radar data or satellite data could not determine the location of the actual eruption site within the caldera. Scientists onboard a flight to Grímsvötn (from 20:20 to 23:05 UTC) estimated the vent to be in the vicinity of the 2004 eruption, but accurate location could not be determined due to cloud cover. Only 15 hours later the vent was determined to be at a similar/same place as the 2004 eruption. However, had the OREL system been in place, one could have seen that the median location of lightning discharges was 2-3 km south of the 2004 vent after only 30 minutes from the start of the eruption. With a simple wind correction the estimate would have indicated a vent at 2 km west-southwest of the 2004 site. After 3 hours, the estimate would have indicated that the eruption site was about 1 km west of the 2004 site. Four hours into the eruption (at 22:00 UTC) the wind corrected estimates are all within 1 km of the actual eruption crater (Figure 23).

The OREL system has two main parts; an E-mail warning system, and a web site presenting results of the location analysis. The real-time lightning data is retrieved by IMO from the UK Met Office every 10 minutes and the mean location analysis is updated. If the onset of a thunderstorm in Iceland is detected or a significant increase in lightning activity is observed, then an E-mail warning message is sent to a select group, including the 24-7 watch at the IMO. These messages are also used by the IMO weather watch to monitor thunderstorms in Iceland. Weather thunderstorms during the summer of 2013 indicate that the response time of the system is 10-20 minutes. The response time reflects the total time from the first lightning strike until the web pages were updated and E-mail warnings sent. The results of the analysis of the system are also published on the web, as a map, graph and tables. The text and labels are in Icelandic, but an English glossary is provided. The web site is currently:

<http://brunnur.vedur.is/athuganir/eldingar/eldgos/>

The main page shows a map with the lightning locations in Iceland during the past 24 hours, color coded in 3 hour bins. Detailed explanations are provided on the web.

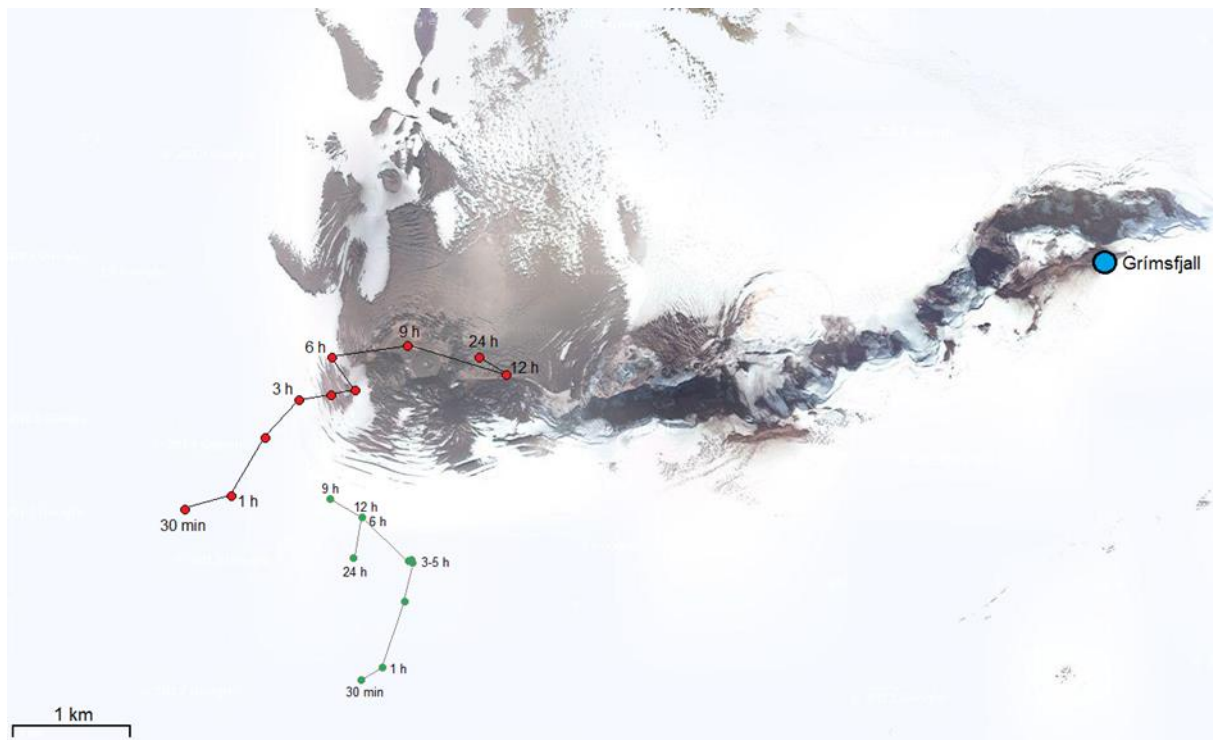


Figure 23 Aerial view of Grímsvötn after the 2011 eruption, with the eruption crater visible in the SW-corner of the caldera (close to the 9 h red dot) about 6 km W of the Grímsfjall station. The eruption site estimates are shown for 0.5, 1, 2, 3, 4, 5, 6, 9, 12 and 24 hours after the onset of the eruption. The green dots indicate the median lightning locations and the red dots show the locations after a simple wind correction with a time constant of 500 s. Four hours into the eruption (at 22:00 UTC) the wind corrected estimates are all within 1 km of the actual eruption crater

To summarize, an automatic monitoring system has been developed that estimates the location of an eruption based on the mean location of real-time volcanic lightning data. The system delivers E-mail warnings and provides a web page with eruption site location estimate. The following should be noted:

- It is possible that mean or median location of lightning may give the best estimate of the eruption site for the early hours of an eruption, especially if darkness, weather and visibility prevent direct observations.
- The initial lightning activity in the volcanic plume may not be sufficient to give useful information. However, for the largest and most dangerous subglacial eruptions, intense early lightning activity is expected.
- For a more accurate eruption site estimate, a wind correction is needed. More work is needed in developing a suitable wind correction.

Additional local ALDF lighting location data could be available at minor additional cost. This data has the potential of providing more accurate eruption site estimates. Therefore, it is important for IMO to finalize the installation of its ALDF lighting location system.

3.2 Analysis of motion in the Eyjafjallajökull plume

The wealth of data gathered in the 2010 eruption of Eyjafjallajökull has been used to examine details of plume dynamics that are relevant for the advancement of plume modeling. A short description of these activities by WP partners follows.

Björnsson et al (2013) analysed data from web-camera captured during the eruption and employed the maximum cross correlation (MCC) method to track motion on the outside of the buoyant part of the plume. Based on this, the vertical velocity was estimated for three intervals during the eruption. Figure 24 shows how the MCC method distinguishes the plume from the background of the image, and shows a snapshot of the plume motion. The temporal evolution of the plume motion was studied using the results of the velocity analysis.

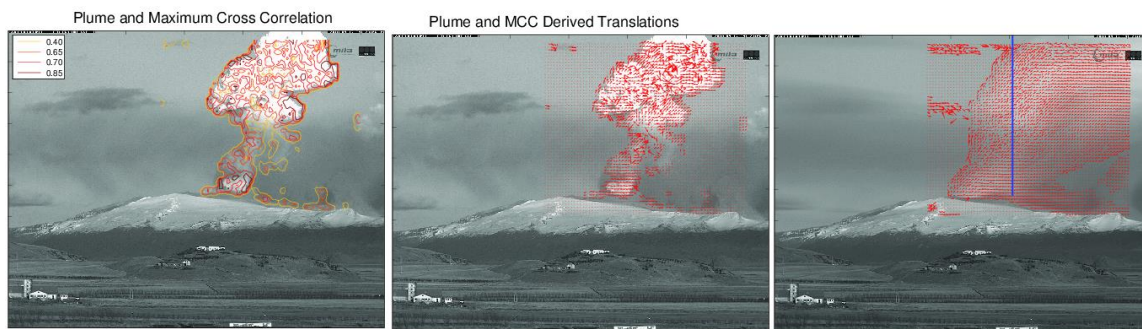


Figure 24 Instantaneous snapshot of the plume and its motion. **Left:** the results of the application of the MCC method on the eruption plume on 17 April at 20:06:44. Only points where the MCC value was higher than 0.4 are shown. **Middle:** translation vectors that show the direction that each point is translated to in the subsequent image, which yields an estimate of the velocity on the exterior of the plume. **Right:** average plume and average exterior motion on 17 April for the period 20:03 – 20:07. The blue line shows the location of the transect in Figure 25.

The results show that in the buoyant part of the plume, on average there were updrafts in one part of the cloud and lateral motion or downdrafts in another. Even within the regions of updraft in the plume, there are alternating motions of strong updrafts, weak updrafts and downward motion. These results show a highly variable plume driven by intermittent explosions. Thus, instead of a steady or slowly varying source, giving rise to a plume with a well-defined vertical velocity profile, the results suggest a plume driven by intermittent explosions of varying strength followed by strong updrafts and fast rising cloud turrets. Figure 25 shows an example of this, together with 5 minute averages of the vertical velocity on the exterior of the plume from 1500-2100 UTC on 17 April. While the average vertical velocity profile during the entire 6 hour period has a well-defined structure, there is considerable scatter in the 5 minute averages, due to the intermittent behaviour of the plume.

Ripepe et al (2013) used thermal images and infrasound data to analyze temporal variations of the plume on 4 May. They find the plume is maintained by thermal puffs with velocities varying from 50 – 140 m/s at the vent (see Figure 26).

These results, along with other recent papers on the Eyjafjallajökul eruption (Bonadonna et al 2011) highlight the intermittent behaviour of the plume. The conceptual picture that arises is different from the one underlying classical plume models, in that instead of a steady or slowly varying source, giving rise to a plume with a well-defined vertical velocity profile, the results suggest a plume driven by intermittent explosions of varying strength. For the dynamics of the plume and the lofting of ash, the puffs and updrafts are of considerable importance.

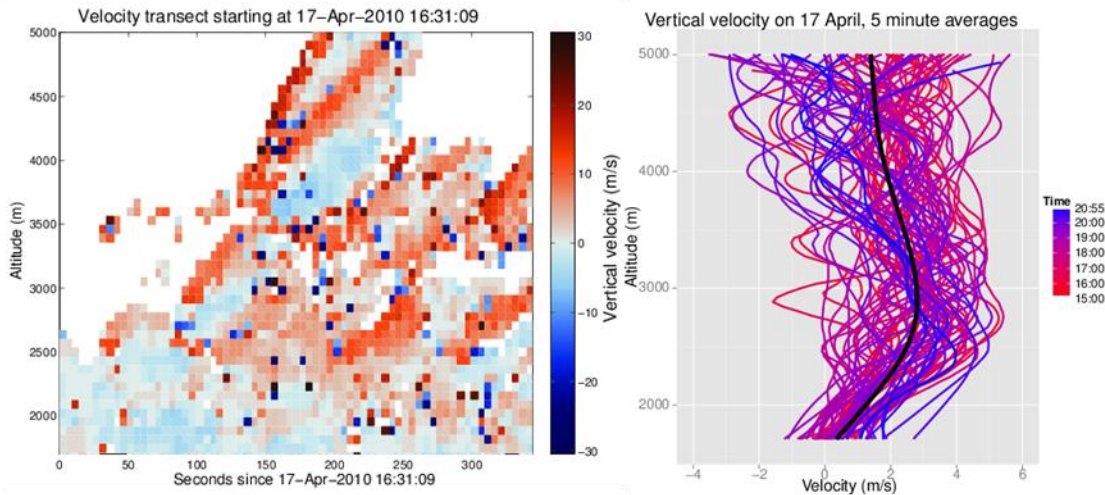


Figure 25 The temporal evolution of motion on the plume exterior (left) along the transect shown in Figure 24. Instantaneous snapshot of the plume and its motion. Left: the results of the application of the MCC method on the eruption plume on 17 April at 20:06:44. Only points where the MCC value was higher than 0.4 are shown. Middle: translation vectors that show the direction that each point is translated to in the subsequent image, which yields an estimate of the velocity on the exterior of the plume. Right: average plume and average exterior motion on 17 April for the period 20:03 – 20:07. The blue line shows the location of the transect in Figure 25.

The results show that in the buoyant part of the plume, on average there were updrafts in one part of the cloud and lateral motion or downdrafts in another. Even within the regions of updraft in the plume, there are alternating motions of strong updrafts, weak updrafts and downward motion. These results show a highly variable plume driven by intermittent explosions. Thus, instead of a steady or slowly varying source, giving rise to a plume with a well-defined vertical velocity profile, the results suggest a plume driven by intermittent explosions of varying strength followed by strong updrafts and fast rising cloud turrets. Figure 25 shows an example of this, together with 5 minute averages of the vertical velocity on the exterior of the plume from 1500-2100 UTC on 17 April. While the average vertical velocity profile during the entire 6 hour period has a well-defined structure, there is considerable scatter in the 5 minute averages, due to the intermittent behaviour of the plume.

Ripepe et al (2013) used thermal images and infrasound data to analyze temporal variations of the plume on 4 May. They find the plume is maintained by thermal puffs with velocities varying from 50 – 140 m/s at the vent (see Figure 26).

These results, along with other recent papers on the Eyjafjallajökul eruption (Bonadonna et al 2011) highlight the intermittent behaviour of the plume. The conceptual picture that arises is different from the one underlying classical plume models, in that instead of a steady or slowly varying source, giving rise to a plume with a well-defined vertical velocity profile, the results suggest a plume driven by intermittent explosions of varying

strength. For the dynamics of the plume and the lofting of ash, the puffs and updrafts are of considerable importance.

The results show that in the buoyant part of the plume, on average there were updrafts in one part of the cloud and lateral motion or downdrafts in another. Even within the regions of updraft in the plume, there are alternating motions of strong updrafts, weak updrafts and downward motion. These results show a highly variable plume driven by intermittent explosions. Thus, instead of a steady or slowly varying source, giving rise to a plume with a well-defined vertical velocity profile, the results suggest a plume driven by intermittent explosions of varying strength followed by strong updrafts and fast rising cloud turrets. Figure 25 shows an example of this, together with 5 minute averages of the vertical velocity on the exterior of the plume from 1500-2100 UTC on 17 April. While the average vertical velocity profile during the entire 6 hour period has a well-defined structure, there is considerable scatter in the 5 minute averages, due to the intermittent behaviour of the plume.

Ripepe et al (2013) used thermal images and infrasound data to analyze temporal variations of the plume on 4 May. They find the plume is maintained by thermal puffs with velocities varying from 50 – 140 m/s at the vent (see Figure 26).

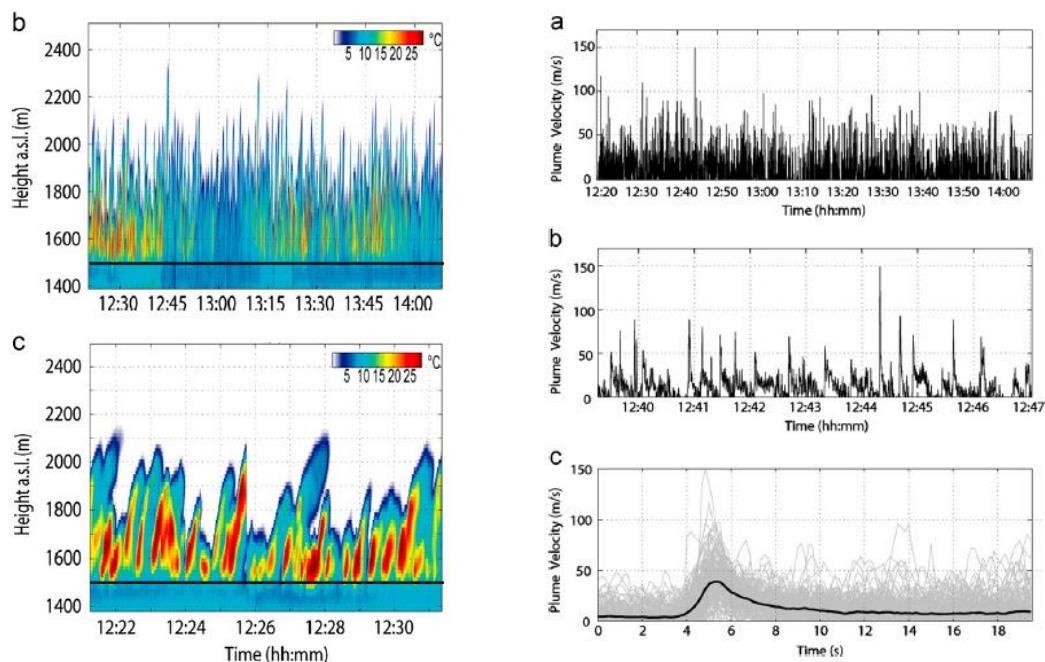


Figure 26 Left, a vertical profile of the plume temperature derived from thermal images taken during a 2.5 hour period on 4 May. The images show that the plume was sustained by thermal puffs reaching 400 – 500 metres above the vent. Right, velocity estimates based on the analysis of the thermal images.

As described in section 2.8, additional cameras have been set up as part of FutureVolc. To deal with an increase in the volume of image and video data collected improvements in the algorithms that characterize motion in the data have been made. These algorithms allow for the real-time quantification of velocity and altitude of identifiable features in the images, and, furthermore, they

can allow for the real-time localization of developing vents during fissure eruptions, and their migration and width.

An example from the Eyjafjallajökull flank eruption is shown in Figure 27, where two vents could be distinguished based on the (anticorrelated) time series of their eruption heights. Current research aims to develop the particle image velocimetry method for improved back tracing of the origin of the vents.

Real time analysis of eruption vent activity (Eyjafjallajökull example)

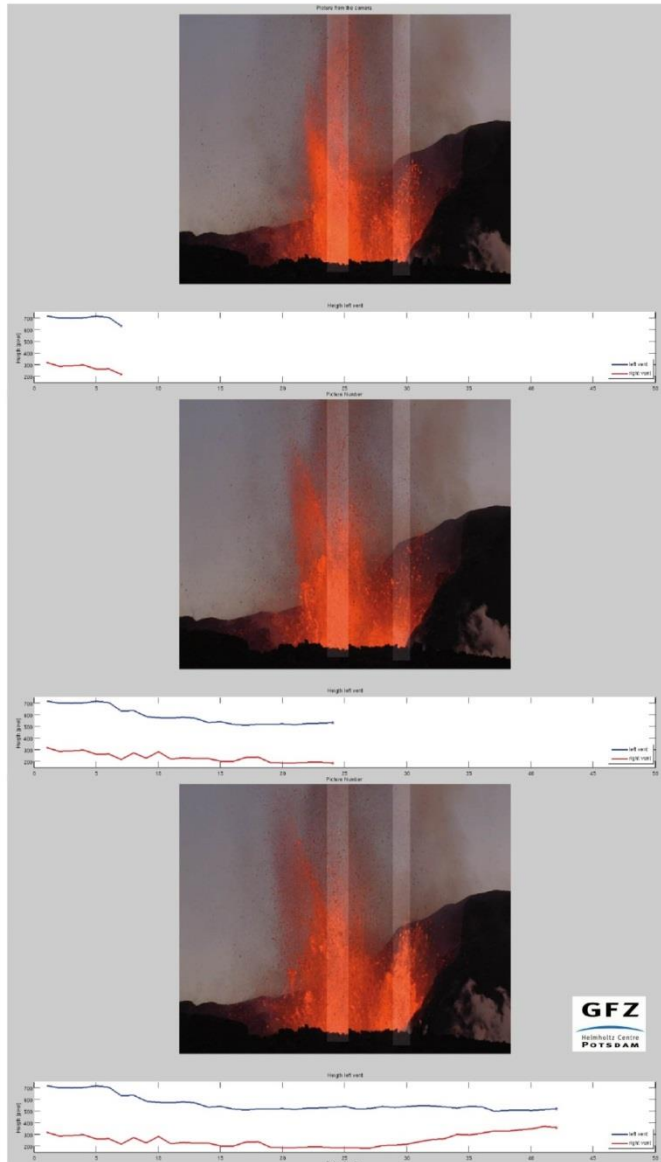


Figure 27 An example from the flank eruption of Eyjafjallajökull. The two vents could be distinguished based on their (anticorrelated) eruption height time series.

3.3 Advances in plume modeling

The entrainment of ambient air as the plume rises is one of the fundamental controls on the height reached by the plume. The entrainment process is affected by both the dynamics of the plume and the atmosphere. The atmospheric controls on plume motion can be a source of error when empirical relationships (Sparks et al, 1997; Mastin et al, 2009), are used to estimate the mass

eruption rate (MER) based on plume altitude. Corrections for the effects of wind have recently been developed (Degruyter and Bonadonna, 2012; Woodhouse et al, 2013) based in part on observations from the Eyjafjallajökull eruption.

Using time series of the altitude of the plume from Eyjafjallajökull, obtained from the C-band radar at Keflavik, and lightning observations of volcanic lightning (ADTnet, (Arason, 2011a) and a lightning mapping array (LMA) of very high frequency receiving stations (Behnke, submitted)), Woodhouse and Behnke (2013, In prep.) are able to assess the predictions of an integral plume model for the trajectories of the plume.

Observations of lightning discharges made by the LMA over a short time interval during the eruption give an indication of the trajectory of the volcanic plume close to the source (typically up to 30 km from the vent). The trajectory can be compared to that predicted using the integral model of volcanic plumes (Woodhouse et al., 2013) with source conditions determined by matching the model plume height to an independent observation from a radar data set (Arason, 2011b). In addition, the growth of the plume as predicted by the model can be compared to the spread of the lightning observations

A typical result of the comparison is shown in Figure 28 and Figure 29. The plume trajectory obtained from the model gives a good description of the observed trajectory (Figure 28), and the plume width prediction from the model provides a reasonably good envelope of the LMA observations. The side view of the plume (Figure 29) shows a high density of LMA data clustered on the lower edge of the plume as the plume bends over. This is consistent with the expectation that solid pyroclasts carry charge, so charge becomes localized as the large pyroclasts begin to fall out of the plume.

The combination of lightning observations with predictions from the volcanic plume model could provide a powerful tool for determining the volcanic source conditions during an eruption. By adjusting source conditions input into the plume model in order to match the model prediction to the observed trajectory and spread of the lightning data, estimates of the volcanic source parameters can be made. The use of a large observational data set such as the LMA data (as opposed to a single observation of the plume height obtained from radar, for example) allows the model prediction to be assessed.

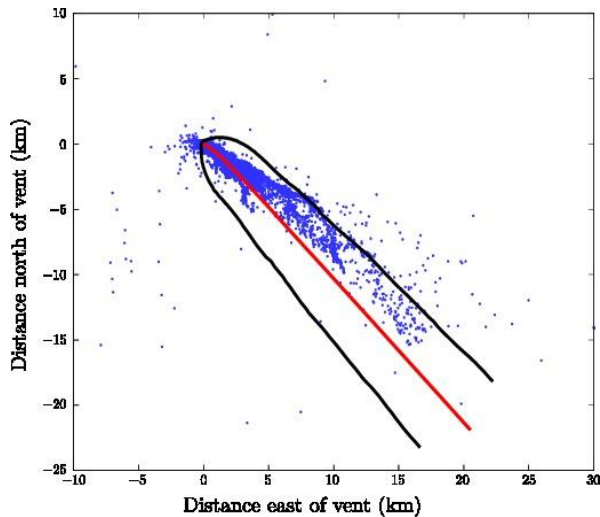


Figure 28 : Plan view of the predicted centreline trajectory (red line) and width (black line) of the plume from Eyjafjallajökull on 11 May 2010 at 2100 UTC, and observations of lightning discharges from the LMA for the period 1900—2100 (blue points)

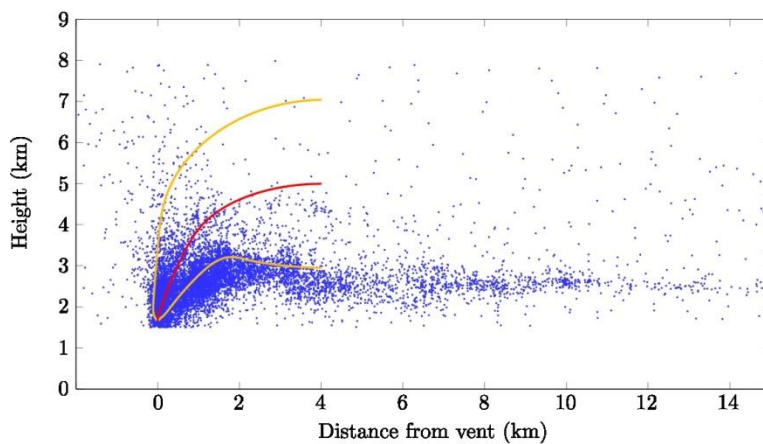


Figure 29 Side view of the predicted centreline trajectory (red line) and upper and lower plume edges (orange lines) of the plume from Eyjafjallajökull on 11 May 2010 at 2100 UTC, and observations of lightning discharges from the LMA for the period 1900—2100 (blue points).

3.4 PlumeRise – an operational webtool for plume modelling

During an eruption there is considerable operational need to make a quick estimate of the mass eruption rate (MER). This estimate has typically been made based on observations of the plume height and various atmospheric parameters. Recently, a model of volcanic plumes has been made available that allows improved MER estimates to be made over the web. This tool, PlumeRise, was designed by Futurvolc partners at the University of Bristol. In the following, this tool is briefly summarised.

A crucial requirement for forecasting ash dispersal is the rate at which material is delivered from the volcano to the atmosphere, a quantity known as the mass eruption rate. It is currently not possible to measure the mass eruption rate directly, so an estimate is made by exploiting a relationship between the mass eruption rate and the height of the plume which is obtained from the fundamental

dynamics of buoyant plumes and calibrated using a dataset of historical eruptions. However, meteorology is not included in the calibrated scaling relationship. Recent studies (Degruyter & Bonadonna, 2012; Woodhouse et al, 2013) show that meteorology, in particular wind conditions, at the time of the eruption has a large effect on the rise of the plume. Neglecting the wind can lead to under predictions of the mass eruption rate by more than a factor of 10 (Woodhouse et al, 2013).

Another recent advance is the development of an improved mathematical model of volcanic plumes that allows detailed meteorological data to be included in the calculation of the plume dynamics. This model can be used to provide estimates of the source mass flux from an observation of the plume height during eruptions.

In order to allow the model to be used during future eruptions, it has been implemented as the PlumeRise web-tool. PlumeRise (www.plumerise.bris.ac.uk) is a free-to-use tool enabling users to perform calculations using input meteorological observations or idealized atmospheric profiles (Figure 30) Volcanic source conditions can be specified and the resulting plume height determined (Figure 31). Alternatively, an inversion calculation can be performed where the source conditions are varied to match the predicted plume height to an observation. Graphical output is produced on completion of calculations and detailed numerical results can be downloaded for subsequent use in atmospheric dispersion models, for example. Multiple runs can be performed to facilitate comparison of different parameter sets, allowing different source and/or meteorological conditions to be assessed.



Figure 30 The PlumeRise modelling page. Source conditions and meteorological data is input into the text boxes. After running the model calculation, graphical data is displayed.

| Parameter set 1 | | Values at plume top | | Values at neutral buoyancy | |
|--------------------------|--|-------------------------|---|----------------------------|--|
| Plume status: | Plume is buoyant | Centreline height: | 7527 m | Centreline height: | 6735 m |
| Source total mass flux: | $2.885 \times 10^6 \text{ kg s}^{-1}$ | Top of plume height: | 10319 m | Mass flux: | $7.235 \times 10^8 \text{ kg s}^{-1}$ |
| Source solids mass flux: | $2.798 \times 10^6 \text{ kg s}^{-1}$ | Mass flux: | $1.191 \times 10^9 \text{ kg s}^{-1}$ | Volume flux: | $7.794 \times 10^8 \text{ m}^3 \text{ s}^{-1}$ |
| Source volume flux: | $4.021 \times 10^6 \text{ m}^3 \text{ s}^{-1}$ | Volume flux: | $1.391 \times 10^9 \text{ m}^3 \text{ s}^{-1}$ | Solids mass fraction: | 0.003867 |
| Source velocity: | 20.00 m s^{-1} | Solids mass fraction: | 0.002349 | Solids volume fraction: | 2.991×10^{-6} |
| Condensation height: | — | Solids volume fraction: | 1.676×10^{-6} | | |
| Parameter set 2 | | Values at plume top | | Values at neutral buoyancy | |
| Plume status: | Plume is buoyant | Centreline height: | 12724 m | Centreline height: | 11303 m |
| Source total mass flux: | $4.327 \times 10^7 \text{ kg s}^{-1}$ | Top of plume height: | 19599 m | Mass flux: | $4.074 \times 10^9 \text{ kg s}^{-1}$ |
| Source solids mass flux: | $4.197 \times 10^7 \text{ kg s}^{-1}$ | Mass flux: | $5.677 \times 10^9 \text{ kg s}^{-1}$ | Volume flux: | $7.634 \times 10^9 \text{ m}^3 \text{ s}^{-1}$ |
| Source volume flux: | $6.032 \times 10^6 \text{ m}^3 \text{ s}^{-1}$ | Volume flux: | $1.257 \times 10^{10} \text{ m}^3 \text{ s}^{-1}$ | Solids mass fraction: | 0.01048 |
| Source velocity: | 300.0 m s^{-1} | Solids mass fraction: | 0.007578 | Solids volume fraction: | 4.660×10^{-6} |
| Condensation height: | 10186 m | Solids volume fraction: | 2.851×10^{-6} | | |

Figure 31 Numerical values characterizing the model solutions are provided for use as initial conditions for atmospheric dispersion models.

The PlumeRise model was developed at the University of Bristol by Mark Woodhouse, Andrew Hogg, Jeremy Phillips and Steve Sparks. The PlumeRise web-tool was developed by Chris Johnson (University of Bristol). The tool has been tested by several of the Volcanic Ash Advisory Centres (VAACs). It is also being used by academic institutions around the world.

4 References

Arason, P., A. J. Bennett and L. E. Burgin (2011a), Charge mechanism of volcanic lightning revealed during the 2010 eruption of Eyjafjallajökull, *Journal of Geophysical Research*, **116**, B00C03, doi:10.1029/2011JB008651.

Arason P., G.N. Petersen & H. Bjornsson (2011b) Observations of the altitude of the volcanic plume during the eruption of Eyjafjallajökull., April—May 2010. *Earth Systems Science Data* 3(1):9 – 17

Behnke S.A., R.J. Thomas, H.E. Edens, P.R. Krehbiel & W. Rison (submitted) The 2010 eruption of Eyjafjallajökull.: Lightning and plume charge structure. *J. Geophys. Res.*

Bennett, A. J., P. Odams, D. Edwards and P. Arason (2010), Monitoring of lightning from the April-May 2010 Eyjafjallajökull volcanic eruption using a very low frequency lightning location network, *Environmental Research Letters*, **5**, 044013, doi:10.1088/1748-9326/5/4/044013.

Bjornsson, H., Petersen, G. N. and Arason, P. (2013) Velocities in the Plume of the 2010 Eyjafjallajökull Eruption, *Journal of Geophysical Research* (conditionally accepted for publication)

Degruyter, W., and C. Bonadonna (2012), Improving on mass flow rate estimates of volcanic eruptions, *Geophys. Res. Lett.*, **39**, L16308, doi:10.1029/2012GL052566.

Gaffard, C., J. Nash, N. Atkinson, A. Bennett, G. Callaghan, E. Hibbett, P. Taylor, M. Turp and W. Schulz (2008), Observing lightning around the globe from the surface, 20th International Lightning Detection Conference, Tucson, Arizona, USA, 21-23 April 2008.

Mastin, L. G., M. Guffanti, R. Servranckx, P. Webley, S. Barsotti, K. Dean, A. Durant, J. W. Ewert, A. Neri, W. I. Rose, D. Schneider, L. Siebert, B. Stunder, G. Swanson, A. Tupper, A. Volentik, and C. F. Waythomas (2009), A multidisciplinary effort to assign realistic source parameters to models of volcanic ash-cloud transport and dispersion during eruptions, *J. Volcanol. Geotherm. Res.*, **186**, 10–21, doi: 10.1016/j.jvolgeores.2009.01.008

Ripepe, M, C. Bonadonna, A. Folch, D. Delle Donne, G. Lacanna, E. Marchetti, A. Höskuldsson (2013), Ash-plume dynamics and eruption source parameters by infrasound and thermal imagery: The 2010 Eyjafjallajökull eruption, *Earth and Planetary Science Letters*, **366**, 112 doi:10.1016/j.epsl.2013.02.005.

Sparks, R. S. J., M. I. Bursik, S. N. Carey, J. S. Gilbert, L. S. Glaze, H. Sigurdsson, and A. W. Woods (1997), *Volcanic Plumes*, John Wiley & Sons, 1 ed., 574 pp., ISBN 0471939013.

Woodhouse, M. J., A. J. Hogg, J. C. Phillips, and R. S. J. Sparks (2013), Interaction between

volcanic plumes and wind during the 2010 Eyjafjallajökull eruption, Iceland, *J. Geophys. Res.*, 118, doi:10.1029/2012B009592.

Woodhouse, M.J. & S.A. Behnke (In prep.) Charge structure in volcanic plumes: a comparison of observations to predictions from an integral plume model for the 2010 eruption of Eyjafjallajökull.